Biochimica et Biophysica Acta 1817 (2012) 1660–1670

Contents lists available at SciVerse ScienceDirect

Biochimica et Biophysica Acta

journal homepage: www.elsevier.com/locate/bbabio

Functional characterization of UCP1 in mammalian HEK293 cells excludes mitochondrial uncoupling artefacts and reveals no contribution to basal proton leak

Martin Jastroch [a,*,1], Verena Hirschberg [b,1], Martin Klingenspor [b]

[a] Institute for Diabetes and Obesity, Helmholtz Zentrum Munich, Ingolstädter Landstr. 1, 85764 Neuherberg, Germany
[b] Molecular Nutritional Medicine, Else Kröner-Fresenius-Zentrum, Technische Universität München, Gregor-Mendel-Str. 2, 85350 Freising-Weihenstephan, Germany

ARTICLE INFO

Article history:
Received 10 January 2012
Received in revised form 22 May 2012
Accepted 28 May 2012
Available online 4 June 2012

Keywords:
UCP1
Human embryonic kidney cell
Adenine nucleotide translocase (ANT)
Proton leak kinetics
Basal proton leak

ABSTRACT

Mechanistic studies on uncoupling proteins (UCPs) not only are important to identify their cellular function but also are pivotal to identify potential drug targets to manipulate mitochondrial energy transduction. So far, functional and comparative studies of uncoupling proteins in their native environment are hampered by different mitochondrial, cellular and genetic backgrounds. Artificial systems such as yeast ectopically expressing UCPs or liposomes with reconstituted UCPs were employed to address crucial mechanistic questions but these systems also produced inconsistencies with results from native mitochondria. We here introduce a novel mammalian cell culture system (Human Embryonic Kidney 293 — HEK293) to study UCP1 function. Stably transfected HEK293 cell lines were derived that contain mouse UCP1 at concentrations comparable to tissue mitochondria. In this cell-based test system UCP1 displays native functional behaviour as it can be activated with fatty acids (palmitate) and inhibited with purine nucleotides guanosine-diphosphate (GDP). The catalytic centre activity of the UCP1 homodimer in HEK293 is comparable to activities in brown adipose tissue supporting functionality of UCP1. Importantly, at higher protein levels than in yeast mitochondria, UCP1 in HEK293 cell mitochondria is fully inhibitable and does not contribute to basal proton conductance, thereby emphasizing the requirement of UCP1 activation for therapeutic purposes. These findings and resulting analysis on UCP1 characteristics demonstrate that the mammalian HEK293 cell system is suitable for mechanistic and comparative functional studies on UCPs and provides a non-confounding mitochondrial, cellular and genetic background.

1. Introduction

Uncoupling protein 1 (UCP1) belongs to the superfamily of mitochondrial anion carrier proteins and resides in the mitochondrial inner membrane of mammalian brown adipose tissue. There is evidence that the 33 kDa-protein forms a dimer and dissipates proton motive force by proton leakage and thereby accelerates substrate oxidation in the absence of ATP-synthesis. This futile cycle results in heat production which is used to drive non-shivering thermogenesis, a physiological trait that defends the body temperature of small mammals, hibernators and human infants [1]. UCP1 is activated by free fatty acids and inhibited by physiological concentrations of purine nucleoside di- and triphosphates [2,3]. Although these modulators of UCP1 activity have been known for more than 30 years, it is still controversial how they structurally interact with UCP1. These crucial mechanistic questions are not only important to the biological understanding of mitochondrial uncoupling and non-shivering thermogenesis, but will also assist to assess UCP1 as a therapeutic target. Brown adipose tissue has been re-discovered as a therapeutic tool for diseases such as obesity and diabetes in humans [4–7]. Although there are major efforts to increase brown adipose tissue mass [8,9], one also has to consider the activation of brown adipose tissue which is under complex central nervous control. Biochemical and biophysical insights on mechanisms of UCP1 activity will become instrumental to allow direct pharmacological intervention, thereby circumventing physiological control of brown adipose tissue.

There is an ongoing debate whether protons are directly channelled by UCP1, or how fatty acids contribute to net proton transport of UCP1 (reviewed in [10]). Furthermore, it is discussed whether purine nucleotide-inhibited UCP1 contributes to unregulated basal proton leak [11,12].

Much of the controversy on the molecular mechanisms underlying UCP1 function derives from inconsistent results in different experimental systems and laboratories. Studies on reconstituted UCP1 in liposomes failed to convincingly address crucial molecular functions as many of these results were not reflected in isolated mitochondria. This includes whether ubiquinone is an obligatory cofactor for UCP1 function, whether fatty acids are required for UCP1 activity and how they interact with UCP1 [13,14]. Liposomal studies of different laboratories obtained contradicting results considering UCP1 activity, the role of fatty acids [15,16], activator specificity [13,15] and the dependence on membrane potential [17,18].

In isolated yeast mitochondria, mouse UCP1 ectopically expressed at a low level shows native behaviour in respect to fatty acid and purine

* Corresponding author. Tel.: +49 89 3187 2105; fax: +49 89 3187 3799.
E-mail address: martin.jastroch@helmholtz-muenchen.de (M. Jastroch).
[1] These authors contributed equally to this study.

0005-2728/$ – see front matter © 2012 Elsevier B.V. All rights reserved.
doi:10.1016/j.bbabio.2012.05.014

nucleotide responsiveness. Unfortunately, UCP1 in yeast displays artificial, purine nucleotide-insensitive uncoupling at concentrations above 1 μg per mg mitochondrial protein which is about 15 to 20% of the protein levels that are found in brown adipose tissue mitochondria from warm-acclimated mice [19]. Further inconveniences of the yeast system include the extrapolation of yeast UCP1 activity to 37 °C for comparison with brown adipose tissue mitochondria using a vaguely assumed Q_{10} value of 2 for the proton leak process [19]. Other functional properties of UCP1 may also be affected in this fungal, non-animal cellular background, and potential cofactors might be missing as suggested by others [20].

Numerous studies on UCP1 structure–function relationships using site-directed mutagenesis were performed in liposomes and yeast, but unequivocal conclusions on the function of conserved residues are hampered by non-native properties of UCP1 in these systems. Unfortunately, the structure of UCP1 is unknown and therefore, protein integrity upon mutation cannot be confirmed.

It appears that UCP1 knockout mice provide an excellent system to investigate the function of UCP1 in its native environment. While the peculiarities of UCP1 knockout mice breeding and the limited amounts of brown adipose tissue prevent high-throughput approaches, the murine knockout system has a pivotal role to validate observations in other experimental systems. The UCP1 knockout mouse is probably the best established system so far, but the deletion of UCP1, a central protein for thermogenesis and energy balance, may provoke unwanted compensatory mechanisms during mouse ontogeny. These secondary effects of UCP1-ablation include thermogenesis in other tissues [21], mitochondrial adjustments in response to oxidative stress in brown adipose tissue [22] and biophysical changes in mitochondrial properties monitored as swelling [23]. Although the UCP1 knockout mouse is well-established for physiological questions, it may not be a robust system for functional assays. This is further corroborated by recent attempts to address whether UCP1 contributes to basal proton leak. Parker and colleagues show that brown adipose tissue mitochondria from UCP1 knockout as compared to wildtype mice have an increased basal proton leak [11], but this has been refuted by others [12]. Shabalina and colleagues demonstrated that some experimental conditions are selectively detrimental for UCP1 knockout mitochondria, thereby implicating that the mitochondrial background has changed in response to the loss of UCP1, which complicates functional assays on UCP1 [12].

Immortalised mammalian cells are a powerful tool to study the function of an ectopically expressed target protein [24]. Surprisingly, this system has been rarely used to assess molecular mechanisms and acute regulation of UCPs. In a promising study by Casteilla and colleagues UCP1 was expressed in Chinese hamster ovary cells (CHO) and GDP-sensitivity of UCP1 was demonstrated [25]. Unfortunately, the authors just show exemplary traces on mitochondrial oxygen consumption and membrane potential. These traces indicate that UCP1 is not fully inhibited in the presence of GDP, as oligomycin-insensitive respiration appears to be higher and membrane potential is lower in UCP1-containing CHO mitochondria when comparing to the wildtype traces. A later study reports that the UCP1 CHO clones express roughly 1 μg UCP1 per mg mitochondrial protein, which approximates the range of functional UCP1 in yeast [26].

In the present study, we introduce a novel mammalian cell system which stably expresses UCP1 in HEK293 cells. Most importantly, we demonstrate that ectopically expressed UCP1 does not display artificial uncoupling and that catalytic centre activities reflect values of native UCP1.

2. Material and methods

2.1. Cell culture

Human embryonic kidney cells (HEK293) were cultured in Dulbecco's Modified Eagle Medium (4500 mg/l glucose, + L-glutamine, − pyruvate) supplemented with 10% foetal calf serum (Biochrom), 50 μg/ml gentamycin and 2.5 μg/ml amphotericin B at 37 °C in a 5% CO_2 humidified incubator. For passaging, cell medium was removed, the cells washed with PBS and trypsinised (0.2% trypsin). Detached cells were suspended in medium, centrifuged (500 *g*; 3 min), re-suspended in growth medium and seeded on new plates.

2.2. Stable transfection of HEK293 cells

The coding sequence of mouse UCP1 (NM009463) was cloned into a pcDNA3 vector (Invitrogen). HEK293 cells with stable expression of mouse UCP1 were generated by calcium-phosphate mediated transfection and subsequent antibiotic selection for stably transfected cells. For this, HEK293 cells were grown up to 60–70% confluency and supplied with fresh medium. The vector DNA was precipitated by mixing the DNA with calcium chloride and Hepes buffered saline (Profection mammalian cell transfection system; Promega) and precipitates were slowly added to the cells. After a 24 h incubation, remaining DNA complexes were washed off and the cells were supplied with fresh medium. Two days post transfection, cells were transferred and diluted on new plates to approximately 25% confluency. To select for positively transfected cells, geneticin (400 μg/ml cell medium; GIBCO) was added for 2 weeks, replacing geneticin-containing medium every 2–3 days. Resulting clonal cell colonies were isolated and separately grown. The expression of UCP1 was verified by immunological detection. Several aliquots of a clonal cell line were stored in liquid nitrogen to control for passaging effects.

2.3. Cellular oxygen consumption

For the analysis of cellular oxygen consumption cells were grown on a 10 cm culture plate to 80% confluence. Growth medium was removed and cells were washed with PBS and detached from the plate with trypsin–EDTA solution. The cell number was determined with a hemocytometer and cells were pelleted by centrifugation and resuspended in 4 ml DMEM containing 10% FBS. The suspension was kept at 37 °C until the analysis of respiration. 1 ml of the cell suspension was transferred to a 4 ml plexi-glass chamber on top of a Clark-type oxygen electrode and saturated with oxygen before the chamber was closed with a lid for the subsequent recording of basal respiration. Leak respiration was induced by addition of 1 μM oligomycin and sensitivity of leak respiration to fatty acids was tested by three additions of 100 μM palmitate. Afterwards FCCP was added until maximum substrate oxidation capacity was reached. The average of 2 aliquots was used as respiratory value for each condition per cell culture plate. Cells from one 1 ml aliquot were spun down and kept for immunological analysis.

2.4. Cell culture for mitochondrial isolation and proton leak measurements

For proton leak measurements, an aliquot of UCP1 expressing and wildtype cells was seeded on a 10 cm cell culture dish. After 3 days the cells were transferred to four 10 cm dishes and on day 5 seeded on two 500 cm^2 dishes. On day 7, the cell medium was replaced and after two more days, the cells were harvested for mitochondrial isolation.

2.5. Isolation of mitochondria from HEK293 cell culture

Mitochondria were isolated by homogenisation and subsequent differential centrifugation. All steps were performed on ice or at 4 °C. Cell medium was removed and the cell layer was washed with 10 ml STE medium (250 mM sucrose, 5 mM Tris, 2 mM EGTA; pH 7.4 at 4 °C). Cells were scraped with a rubber policeman in STE and transferred to a tube for centrifugation (500 *g*; 5 min). The cell pellet was transferred to a dounce homogenizer (WHEATON, 40 ml) and cells were disrupted by seven strokes with a medium-fitted plunger. The homogenate was

centrifuged at 1000 *g* for 10 min and the supernatant was filtered through 250 μm diameter gauze. While the supernatant was transferred to a new centrifuge tube and spun at 10,400 *g* for 10 min to pellet the mitochondrial fraction, the cell pellet was homogenised again and centrifuged at 1000 *g*. The mitochondrial pellet of the fast-spin was resuspended in STE, the supernatant of the second homogenisation was filtered, and both suspensions were centrifuged at 10,400 *g* for 10 min. Both pellets were resuspended, the suspensions combined and centrifuged at 10,400 *g* for 10 min. The final mitochondrial pellet was carefully resuspended in a minimal volume of STE and the mitochondrial protein concentration quantified using the Bradford method (resulting in about 6–14 mg mitochondrial protein from two confluent 500 cm^2 dishes, averaging about $7–8*10^7$ cells).

2.6. Recombinant UCP1 standard

A recombinant mouse UCP1 standard was provided by the laboratory of Bruno Miroux, (Université Paris, Institut de Biologie Physico-Chimique). Recombinant UCP1 was expressed in *E. coli* and purified from inclusion bodies with a histidine tag. Protein concentration and purity of the UCP1 standard were determined by separation on a SDS polyacrylamide gel and subsequent Coomassie staining. The Coomassie stain was quantified with the Odyssey system (Licor) and protein concentration was determined with known BSA concentrations. The purity of the UCP1 standard was calculated by dividing the UCP1 band intensity by the total signal intensity of the gel lane.

2.7. Western blotting

For the analysis of UCP1 expression 1 μg of mitochondrial protein and recombinant UCP1 ranging from 1.25 to 40 ng were electrophoresed in a SDS-polyacrylamide gel (12% w/v) and blotted on a nitrocellulose membrane (AMERSHAM). UCP1 was detected using a rabbit antibody raised against hamster (*Phodopus sungorus*) UCP1 (1:50,000) and an IRdye800-conjugated goat anti rabbit antibody (Licor, 1:25,000). Fluorescence signals were detected in the Licor-Odyssey system and quantified with the manufacturer's software.

The UCP1 content in the mitochondrial samples was calculated by interpolation of the standard signal intensities.

2.8. Protein quantification

Protein amount in the mitochondrial samples for proton leak measurements was quantified with the Bradford method. Five microlitres of the mitochondrial sample (diluted 1:6) were mixed with 1 ml of Bradford reagent and incubated for 5 to 10 min, after which the absorbance was measured at 595 nm. Protein concentrations were calculated using STE-dissolved BSA as a standard.

2.9. Mitochondrial oxygen consumption

Oxygen consumption was measured using a Clark-type oxygen electrode (Rank Brothers, U.K.) maintained at 37 °C in KHE medium (120 mM KCl, 3 mM HEPES, 5 mM KH_2PO_4, 1 mM EGTA) containing 0.3% BSA, pH = 7.2 at room temperature. For the measurement of mitochondrial respiration, mitochondria were incubated in KHE at a final concentration of 0.175 mg/ml. Rotenone (8 μM) was added to inhibit influx of endogenous substrates at complex I and respiration was initiated by addition of 6 mM succinate (referred as state 2 respiration). GDP (1 mM) was added to block leak respiration mediated by UCP1 activity. Subsequently, 600 μM ADP was added to activate ATP synthesis (determined as state 3 respiration). Addition of 1 μg ml^{-1} oligomycin inhibits ATP-synthase and the residual respiration rate is due to the mitochondrial proton leak (state 4 respiration). Sequential titration of FCCP was performed to determine maximum substrate oxidation rates.

2.10. Determination of adenine nucleotide translocase (ANT) content

Carboxy-atractylate (CAT) binds and inhibits the ANT with high specificity [27]. Therefore, CAT inhibits phosphorylating respiration (state 3) in the presence of exogenous ADP. The concentration required to fully inhibit state 3 respiration equals the ANT concentration in the sample. Wildtype and UCP1-containing mitochondria (0.2 mg ml^{-1}) were energised with succinate and state 3 respiration established by adding excessive amounts of ADP (1 mM). CAT was titrated at 0.125 nmol steps up to 2.5 nmol per mg mitochondrial protein successively inhibiting state 3 and establishing state 4 respiration. Respiration rate was plotted against CAT concentration. ANT content was determined as the intercept of state 3 and state 4 gradients.

2.11. Measurement of proton leak kinetics

Proton leak kinetics were determined by measuring mitochondrial membrane potential with a TPMP+ sensitive electrode simultaneously with the oxygen consumption. Mitochondria were incubated at a concentration of 0.35 mg ml^{-1} in KHE-containing 0.3% BSA with 8 μM rotenone, 1 μg ml^{-1} oligomycin, and 110 ng ml^{-1} nigericin to abolish ΔpH (and transforming it to membrane potential). The TPMP+ electrode was calibrated with five sequential additions up to 2.5 μM TPMP+. Succinate (6 mM) was added to start the reaction. Oxygen consumption and membrane potential were titrated by additions of malonate up to 7.5 μM. Where indicated, GDP or palmitate was added at the beginning of each run. The TPMP+ binding correction factor was not determined and therefore assumed to be identical between the two mitochondrial populations around 0.35 (as found for most mammalian tissue mitochondria except the liver).

2.12. Data analysis/calculation of UCP1 activities

For the quantitation and comparison of UCP1 content Western blot signals (Figs. 1 and 2) and their images [28] were densitometrically analysed using Image J (NIH, http://rsbweb.nih.gov/ij/).

For comparison with proton leak data from other studies [11,19,29–32] UN-SCAN-IT software (Version 6.1) was used to digitalise data and subject them to regression analysis using SigmaPlot 11.0 (Systat Software GmbH).

Differential UCP1-activity curves were generated by numeric subtraction using spread sheet software (Excel, Microsoft).

2.13. Statistics

UCP1 protein expression, respiration and proton leak data were tested for statistical differences using Student's *t*-test and plotted as mean values ± standard error. Differences in cellular and mitochondrial respiration states were tested by two-way ANOVA. Data were log-transformed, if appropriate, to meet the requirements of equal variance and normality. Significant differences of $p<0.001$ are indicated by an asterisk or described as significantly different.

3. Results

3.1. Quantitative assessment of UCP1 protein levels in UCP1-expressing HEK293 cells

First, we determined the purity of our recombinant UCP1 standard by staining electrophoresed recombinant UCP1 samples with Coomassie. Dividing the intensity of the UCP1 band by the intensity of the total lane gives a 60.7% purity of recombinant UCP1 (Fig. 1A). We then confirmed that our anti-hamster UCP1 antibody detects recombinant mouse UCP1 (Fig. 1B) in a linear range from 0 to 40 ng of UCP1 protein (Fig. 1C). Next, we determined the mouse UCP1 content in isolated mitochondria of a stably transfected HEK293 cell line. We found 4.8 ± 0.3 μg

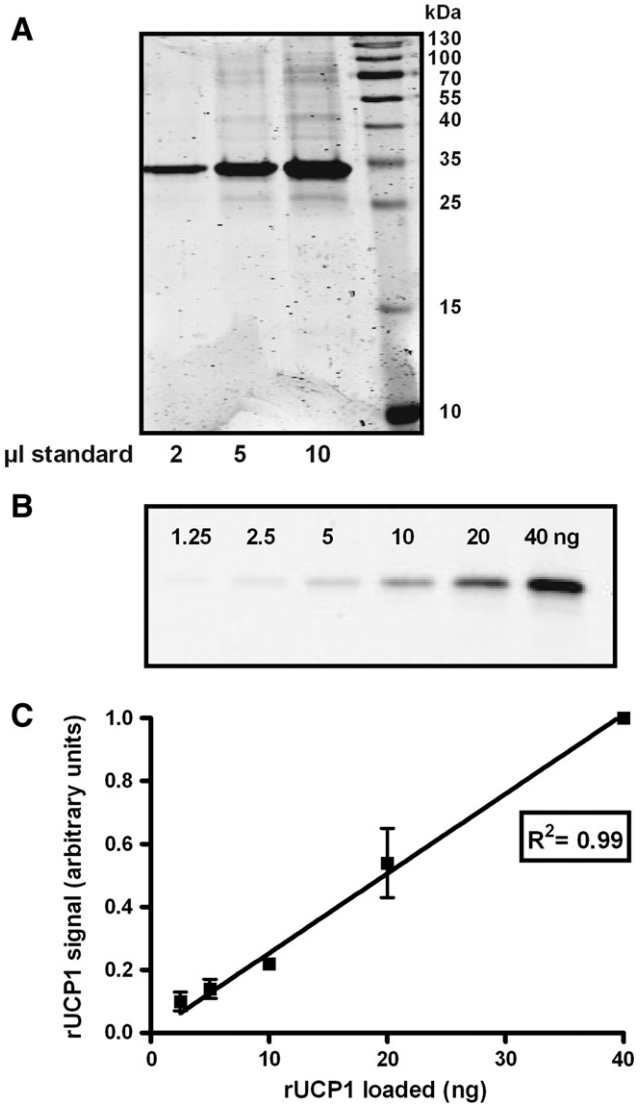

Fig. 1. Determination of UCP1 standardisation. (A) Calculation of standard purity. Recombinant UCP1 was separated on a SDS gel, stained with Coomassie and analysed with an infrared imaging system (Licor, Odyssey). Purity of 60.7% was calculated by dividing the UCP1 band intensity with the total lane intensity and averaged for three different loading amounts. (B) Western blot detection of recombinant UCP1 with a polyclonal antibody against hamster UCP1. (C) Linearity of calibration standard. UCP1 standards were run on different gels, signals were normalised to the signal for 40 ng. Densitometric signals were proportional to loaded UCP1 amount. Values are means ± SEM, n = 5.

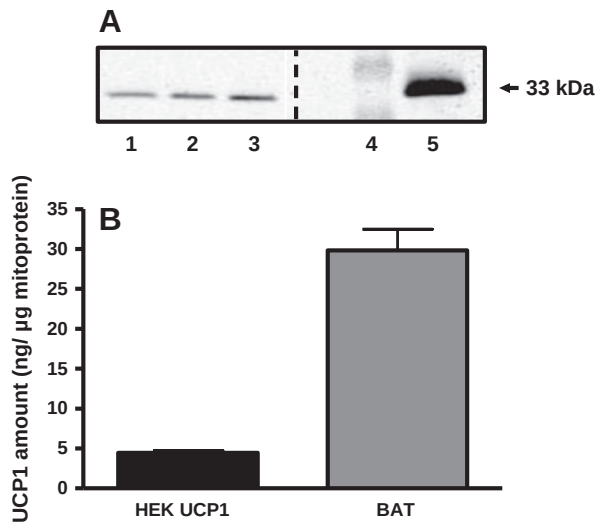

Fig. 2. Immunodetection of UCP1 in isolated HEK293 cell mitochondria. (A) Example for immunodetection of UCP1 showing three independent mitochondrial preparations from HEK293 UCP1 cells (lanes 1–3) run with a mass standard (lane 4) and BAT mitochondria from mice kept at 22–24 °C as reference (lane 5). (B) Quantification of UCP1 protein content in HEK293 cell and mouse BAT mitochondria. Specific signals for UCP1 from different mitochondrial preparations were analysed densitometrically. Using purified recombinant UCP1 protein standard, a calibration curve was constructed and UCP1 content of the samples was calculated. Bars represent means ± SEM, n = 3.

UCP1 per mg mitochondrial protein in the transfected HEK293 cell line (Fig. 2A, n = 5). No UCP1 protein was detected in wildtype HEK293 mitochondria. In comparison, brown fat mitochondria of C57BL/6 (B6) mice kept at 22–24 °C contain 29.8 ± 2.6 µg UCP1 mg^{-1} mitochondrial protein (Fig. 2A, n = 3), while 6.3 µg UCP1 mg^{-1} mitochondrial protein was reported in mice acclimated to thermoneutral temperatures [19]. Finally, we calculated that thymus mitochondria from B6 mice possess about ten times less UCP1 than BAT mitochondria [28], therefore containing about 3 µg UCP1 mg^{-1} mitochondrial protein.

3.2. Cellular and mitochondrial respiration

Then, we compared respiration of UCP1-containing and wildtype trypsinised cells and mitochondria (Fig. 3). In glucose- and serum-containing cell media, basal respiration between the two cell lines was not significantly different, while proton leak respiration in the presence of 1 µM oligomycin was significantly lower in wildtype cells (Fig. 3A). Addition of palmitate increased the difference between UCP1-containing and wildtype cells. Also, palmitate induced the respiration significantly as compared to oligomycin-dependent respiration in UCP1-containing but not in wildtype cells. Cellular respiration in the presence of FCCP was not different between the two cell-types. In isolated mitochondria, non-phoshorylating respiration with succinate (state 2) was twice as high in UCP1-containing mitochondria as compared to wildtype mitochondria. The administration of GDP significantly decreased state 2 respiration in UCP1-containing cells. Phosphorylation was induced by the administration of excessive ADP (600 µM) and was significantly higher in UCP1-containing mitochondria. After addition of oligomycin to inhibit ATP synthesis, respiration rates reporting proton leak (state 4) were indistinguishable between UCP1-containing and wildtype mitochondria. FCCP-respiration rates were not significantly different between mitochondria of both cell lines.

3.3. Regulation of UCP1 activity in HEK293 cell mitochondria

Next, we measured the proton leak kinetics of UCP1-containing and wildtype mitochondria, as respiration is just a vague indicator of membrane proton permeability. The curve of UCP1-containing mitochondria was shifted upwards as compared to wildtype mitochondria, indicating basal uncoupling activity (compare Fig. 4A and B). This UCP1 activity is most likely mediated by residual fatty acids and the condition was therefore termed 'low fatty acids'. Addition of 100 µM palmitate ('high fatty acids' condition) increases proton conductance selectively in UCP1-containing mitochondria, therefore demonstrating inducible activity of UCP1. At the highest common potential of 123.9 ± 5.5 mV, the proton leak rate, measured as oxygen consumption rate during non-phosphorylating condition, was about 4.5-fold elevated. The presence of 1 mM GDP prevented this activation of UCP1, demonstrating purine nucleotide inhibition of UCP1 in HEK293 mitochondria. Addition of 100 µM palmitate did not significantly affect proton leak kinetics of wildtype HEK293 mitochondria (Fig. 4B).

3.4. Basal proton leak of mitochondria isolated from HEK293 and HEK293 UCP1 cells

In the presence of 100 µM palmitate and 1 mM GDP, the proton leak curve of UCP1-containing HEK293 mitochondria was located

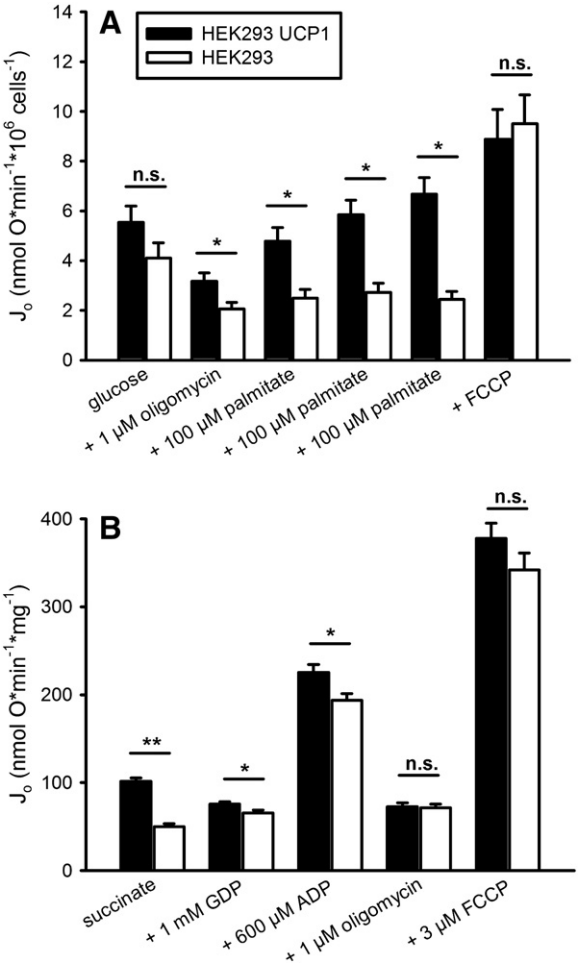

Fig. 3. Respiration of trypsinised wildtype HEK293 and HEK293 UCP1 cells and isolated mitochondria. (A) Cellular respiration of trypsinised HEK293 and HEK293 UCP1 cells was analysed in a Clark electrode. Basal respiration in glucose-containing cell medium with FBS was recorded and subsequently, oligomycin was added to inhibit ATP synthase and establish leak respiration. Fatty acid-sensitivity of leak respiration was tested by additions of each 100 µM palmitate and maximum cellular substrate oxidation was induced by addition of the uncoupler FCCP. Bars represent the mean absolute oxygen consumption of 10^6 cells ± SEM, n = 11–12. (B) Isolated mitochondria were characterized by titration of different respiratory states. Succinate induced non-phosphorylating respiration, which reached basal values by addition of 1 mM GDP. Phosphorylating respiration was determined after addition of ADP and basal leak respiration by addition of oligomycin. Titration of FCCP revealed maximum respiratory capacity of the mitochondria. Bars represent means ± SEM, n = 11–12.

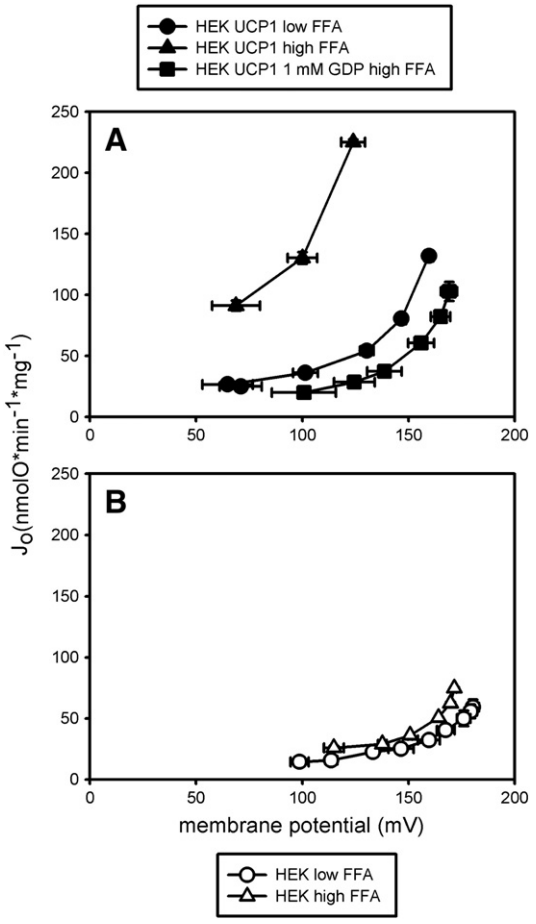

Fig. 4. Modulation of UCP1 uncoupling activity in HEK293 cell mitochondria. Proton leak kinetics of mitochondria isolated from HEK293 UCP1 (upper graph, black symbols) and normal HEK293 cells (lower graph, white symbols). Addition of 100 µM palmitate (triangles) increases proton conductance in mitochondria from HEK293 UCP1 cells, but not in mitochondria from control cells. Addition of 1 mM GDP prevents this increase in proton conductance and re-couples UCP1- containing mitochondria (squares). Under basal conditions (low FFA, circles), the proton leak is higher in UCP1-containing compared to HEK293 wildtype mitochondria.

between the UCP1 low fatty acid and the wildtype curves, suggesting that UCP1 catalyses residual uncoupling. In order to investigate whether this is artifactual uncoupling, similar to what is found in yeast mitochondria ectopically expressing UCP1, we applied more stringent re-coupling conditions by just adding 1 mM GDP without palmitate. We found that 1 mM GDP re-coupled UCP1-containing mitochondria, and completely shifts the proton leak kinetics to wildtype levels, suggesting full inhibition of UCP1 (Fig. 5).

3.5. ANT content

The identity of basal proton leak kinetics between UCP1-containing and wildtype mitochondria may be coincidental as the expression of other mitochondrial carrier proteins could be influenced by ectopic expression of UCP1. In particular the ANT is a candidate as 1) it contributes to basal proton leak [33] and 2) the expression of UCP1 interfered with mitochondrial ADP/ATP balance (Fig. 3, state 3 respiration). In order to exclude that a difference in ANT content causes an over- or underestimation of the UCP1-independent basal proton leak, we measured the ANT content in both cell lines by CAT titration. We found that both cell lines had identical concentrations of ANT approximating 0.7 to 0.8 nmol mg^{-1} mitochondrial protein (Fig. 6).

3.6. Quantification of the catalytic centre activity of UCP1 in different cell systems

We calculated and compared the dimer catalytic centre activity of UCP1 in our HEK293 cell system and other published data (see Table 1). We slightly corrected the values of Stuart et al. [19] by using 33 kDa as the molecular weight of UCP1, deduced from the annotated mouse protein sequence. In contrast to Stuart et al. [19], we calculated the UCP1 activities at the physiologically relevant temperature of 37 °C. For direct comparisons with the yeast system, the yeast proton conductance values were extrapolated to 37 °C using Stuart et al.'s Q_{10} value of 2.

We found that UCP1 in HEK293 cells resembled catalytic centre activities as found for UCP1 in brown adipose tissue mitochondria. The deviations of UCP1 activity in HEK293 mitochondria increased towards higher BSA concentrations up to 4%. The UCP1 activity in

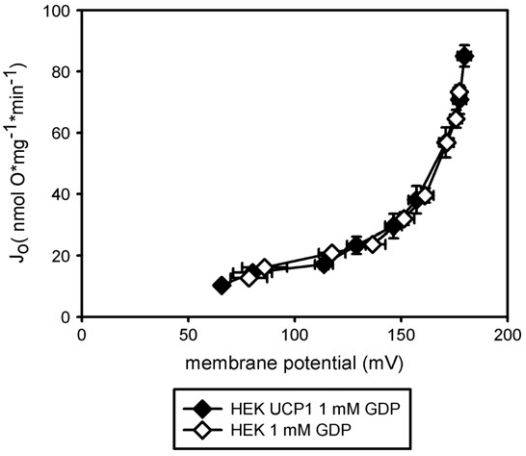

Fig. 5. UCP1 expression in HEK293 cells does not cause an uncoupling artefact. Proton leak kinetics of mitochondria isolated from wildtype HEK293 (white symbols) and UCP1 HEK293 (black symbols) cells in the presence of 1 mM GDP. 1 mM GDP fully inhibits UCP1, leading to an overlay of wildtype and UCP1 proton leak curves. The complete overlay of the curves excludes any artifactual uncoupling of mouse UCP1 in HEK293 cells and suggests that UCP1 does not contribute to basal proton leak.

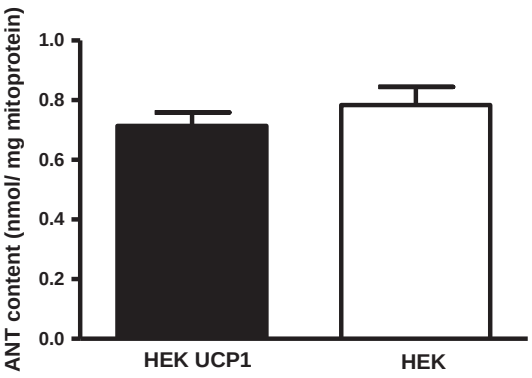

Fig. 6. UCP1 expression does not affect ANT content. ANT content of wildtype HEK293 and UCP1 HEK293 mitochondria was determined by titration with CAT. Five independent measurements for each type of mitochondria revealed that the abundance of this carrier is not altered by stable expression of UCP1 in HEK293 cells. Values are means ± SEM, n = 5.

HEK293 remained, however, between 6 and 12 fold below activities that were found in yeast (Table 1).

3.7. Modelling of the membrane potential-dependent proton leak by regression analysis

To characterize UCP1 activity, we conventionally compared proton leak rates at two arbitrarily selected membrane potentials (see Table 1). However, as UCP1 activity apparently changes over the range of membrane potentials, the attempt to quantify UCP1 activity at a selected membrane potential is limited. Therefore, relating UCP1-activity mathematically as a function of mitochondrial membrane potential allows calculating the full kinetic response of UCP1 activity in mitochondria. In order to do this, the current–voltage (proton leak rate–membrane potential) relationships require biophysical understanding, which is, however, controversially debated. It has been suggested by Garlid et al. [34] that a simple exponential equation sufficiently explains ion transport over an energised membrane, based on the Eyring theory [35]. Others observed ohmic behaviour of proton leak rates at low membrane potential (e.g. [36]), which is supported by numerous biophysical studies on bilayer membranes (e.g. [37]). To test both assumptions, we subjected our data and data depicted from selected publications studying UCP1 to regression analysis. We applied the dynamic fit of a simple 2-factor exponential function ($f(x) = a * \exp^{(bx)}$), as well as a function combining a 2-factor exponential term with a linear term accounting for ohmic behaviour of current–voltage relationships ($f(x) = ax + b * \exp^{(cx)}$, $a > 0$; $c > 0$). We found that our data are supported by $f(x) = ax + b * \exp^{(cx)}$ with a coefficient of determination $R^2 \sim 0.97$ (Supplementary Table). Using simple exponential equations, we observed a stronger deviation of data points in the lower membrane potential range, and an average coefficient of determination $R^2 \sim 0.93$. Testing a 4-factor exponential term (see Supplementary Table), we found a similar coefficient of determination as for the mixed term.

We verified a consistently higher fit of $f(x) = ax + b * \exp^{(cx)}$ as compared to the 2- or 4-factor exponential using data from different studies of either brown adipose tissue mitochondria or ectopic UCP1 expression. These studies comprised different methods to obtain mitochondrial membrane potentials such as TPMP+ [11,19,29,30], rubidium [36], or quenched safranine O [32]. In the meta-analysis, we found a better fit of the mixed term as compared to the 4-factor exponential. Fig. 7 shows an example of the curve fits on UCP1-containing HEK293 mitochondria.

3.8. Calculation of UCP1-dependent proton leak rate as a function of membrane potential

Using $f(x) = ax + b * \exp^{(cx)}$, we illustrated the UCP1-dependent proton leak rate as a function of membrane potential by subtracting the proton leak of wildtype HEK293 from UCP1-containing mitochondria at the same experimental conditions (Fig. 8A). UCP1-dependent leak rate increases exponentially at high membrane potentials but remains predominantly linear at lower membrane potentials. Fig. 8B shows the calculated UCP1 proton leak curves for the studies in animals as labelled in the figure, also indicating study-by-study variations. Using our mathematical transformation, the re-analysed data of UCP1-dependent proton leak curves of yeast mitochondria, both measured on the identical strain but in two subsequent studies, are shown in Fig. 8C and illustrate large study-to-study variation [19,29]. Furthermore, illustration of basal proton leak from wildtype yeast mitochondria and UCP1-containing yeast mitochondria (inhibited with GDP) in Fig. 8D reveals differences in basal proton leak (Fig. 8).

In comparison to proton leak rates that were conventionally calculated assuming linearity between two data points, the values calculated from the mathematically derived function deviate marginally (see Table 1).

In Fig. 9, we calculated the catalytic centre activities per μg UCP1. This illustrates that UCP1 in HEK293 mitochondria works within the activity spectrum of UCP1 from native mitochondria at high membrane potentials (Fig. 9A). In contrast, adding the 'low activity' curve of UCP1 from yeast illustrates that these catalytic centre activities are much higher at any given membrane potential (Fig. 9B).

4. Discussion

Different experimental systems have been applied in the past to study UCP1 and the function of other UCP homologues. These experimental systems produced results inconsistent with tissue mitochondria or displayed artificial uncoupling properties, possibly as a result of increased misfolded protein levels.

We searched for experimental systems that are suitable to study uncoupling protein function. In this study, we introduce mammalian HEK293 cells that ectopically express UCP1. We demonstrate that UCP1 in HEK293 does not display artificial uncoupling and resembles catalytic centre activities similar to UCP1 in brown adipose tissue mitochondria. Therefore, the HEK293 cell system is suitable to address crucial mechanistic functions of UCP1, to identify modulators of UCP1 function and to directly compare various UCP family members. Furthermore, the HEK293 cell system may assist to resolve controversy that even appears for mechanistic questions in the UCP1 knockout

Table 1
Catalytic activities of UCP1 at 37 °C.

Data source	Species	Acclimation	Amount UCP1 (μg mg mito. protein^{-1})	(pmol dimer)	BSA conc. (%)	FFA conc.	UCP1 proton leak rate (linearity between data points) (nmol O mg^{-1} min^{-1})	Calculated UCP1 proton leak rate (based on f(x) = ax + b*exp(cx)) (nmol O mg^{-1} min^{-1})	UCP1 proton conductance (nmol H$^+$ mg^{-1} min^{-1} mV^{-1})	Dimer catalytic centre activity (nmol H$^+$ pmol UCP1 dimer^{-1} min^{-1} V^{-1})	UCP1 proton leak rate (linearity between data points) (nmol O mg^{-1} min^{-1})	Calculated UCP1 proton leak rate (based on f(x) = ax + b*exp(cx)) (nmol O mg^{-1} min^{-1})	UCP1 proton conductance (nmol H$^+$ mg^{-1} min^{-1} mV^{-1})	Dimer catalytic centre activity (nmol H$^+$ pmol UCP1 dimer^{-1} min^{-1} V^{-1})
							126 mV				147 mV			
This study	HEK mouse	37 °C	4.8[a]	73	0.3	Low	29 (24[b])	32.5	1.4 (1.1[b])	19.2 (15[b])	117 (53[b])	60.1	4.8 (2.2[b])	65.8 (29.6[b])
						100 μM	211		10.1	138	n/a		n/a	n/a
	Mouse	24 °C	29.83	452										
Collected in Stuart et al. [19]	Rat	Thermoneutral	13[c]	197	1	Low	23	7.9	1.1	5.6	43	17.8	1.8	9.1
	Rat	Cold, 5 °C	56[c]	848	1	Low	172	83.8	8.2	9.7	312		12.7	14.5
	Mouse	Thermoneutral	6.3[c]	95										
	Mouse	Cold	55[c]	833										
Keipert et al. [30]	skm mouse	24 °C	2.1[d]	32	0.3	Low	24.4	18.3	1.2	36	34	44.1	1.4	43.3
Parker et al. [11]	Mouse	24 °C	29.8[a]	452	4	Extremely low	27.3	37.8	1.3	2.9	41	85.5	1.7	3.8
						160 μM	65		3.1	6.9	178		7.3	16.1
Echtay et al. [29]	Rat	25 °C	13[e]	197	1	Low	34.2	29.1	1.6	8.3	56.3	53.5	2.3	11.7
Shabalina et al. [32]	Mouse	Thermoneutral	6.3[e]	95	0.1	Low	48.3	26.4	2.3	24.2	248		10.1	106.6
Stuart et al. [19]	Yeast 307	30 °C	0.9[c]	14	0.1	Low	33.8	19.9	1.6	115	114	79.0	4.7	332
						High	139.9		6.6	417				
Echtay et al. [29]	Yeast 307	30 °C	0.9[c]	14	0.2	Low	113.3	104.2	5.4	260	109	123.4	4.5	318

[a] Data measured in this study.
[b] Data corrected for Biuret method as protein quantification; UCP1 molecular weight is 33 kDa.
[c] Data from Stuart et al. [19].
[d] Assumed from Neschen et al. [31].
[e] Assumed based on thermoneutral animals in Stuart et al. [19].

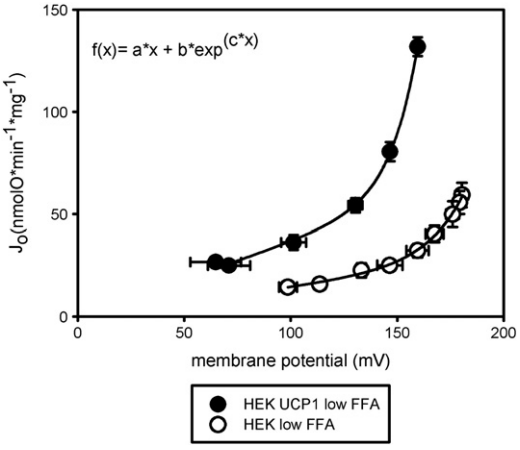

Fig. 7. Regression of proton leak kinetics from HEK293 cell mitochondria. Proton leak curves generated with HEK293 and HEK293 UCP1 mitochondria were best-fitted by a function combining a 2-factor exponential term with a linear term: $f(x) = a*x + b*\exp^{(c*x)}$. R^2 for regressions averaged 0.97 ± 0.02.

mouse model by providing an identical biological background that is unaffected by complex physiological adjustments and compensation during the distorted life history of UCP1-ablated mice.

We first quantified the UCP1 concentration in HEK293 mitochondria (Figs. 1 and 2). This concentration is slightly below the concentration found in brown adipose tissue mitochondria from warm-acclimated rodents [19] and about six times lower than concentrations in mice acclimated to room temperature (Fig. 2). The UCP1 concentration of stably transfected HEK293 mitochondria is, however, well in the physiological range as the UCP1 concentration in mouse thymus mitochondria is about 40% lower than in our UCP1-HEK293 line [28]. Notably, the HEK293 UCP1 concentration is about five times higher than the concentration of functional UCP1 in yeast mitochondria.

Studying respiration in trypsinised, intact cells, we found increased proton leak respiration of UCP1-containing cells as compared to wildtype cells (Fig. 3A) that is possibly due to residual fatty acids in the serum-containing cell medium. Increase of leak respiration rates by addition of palmitate indicates activation of UCP1, while there was no effect on HEK293 wildtype cells. No differences in FCCP-induced respiration demonstrate that the maximum substrate oxidation capacity of the HEK293 cells is unchanged upon ectopic expression of UCP1. In isolated mitochondria, respiration of succinate was higher in UCP1-containing mitochondria, reflecting residual activity of UCP1. GDP decreased the difference, suggesting inhibition of UCP1, and upon addition of oligomycin, respiration rates were indifferent between mitochondria of the two cell lines. Maximum succinate respiration capacity was also not different between UCP1-containing and wildtype mitochondria. For precise characterization of UCP1 function, we measured respiratory fluxes (mitochondrial respiration) simultaneously with steady states of proton motive force (mitochondrial membrane potential).

Here, we demonstrated that UCP1 in HEK293 mitochondria can be activated by fatty acids and inhibited by purine nucleotides (Fig. 4). Importantly, UCP1-dependent proton leak rate could be completely inhibited as compared to wildtype HEK293 mitochondria (Fig. 5). This contrasts the yeast system where UCP1 concentrations above 1 μg per mg mitochondrial protein led to artificial uncoupling [19]. The authors concluded that a higher rate of protein synthesis may

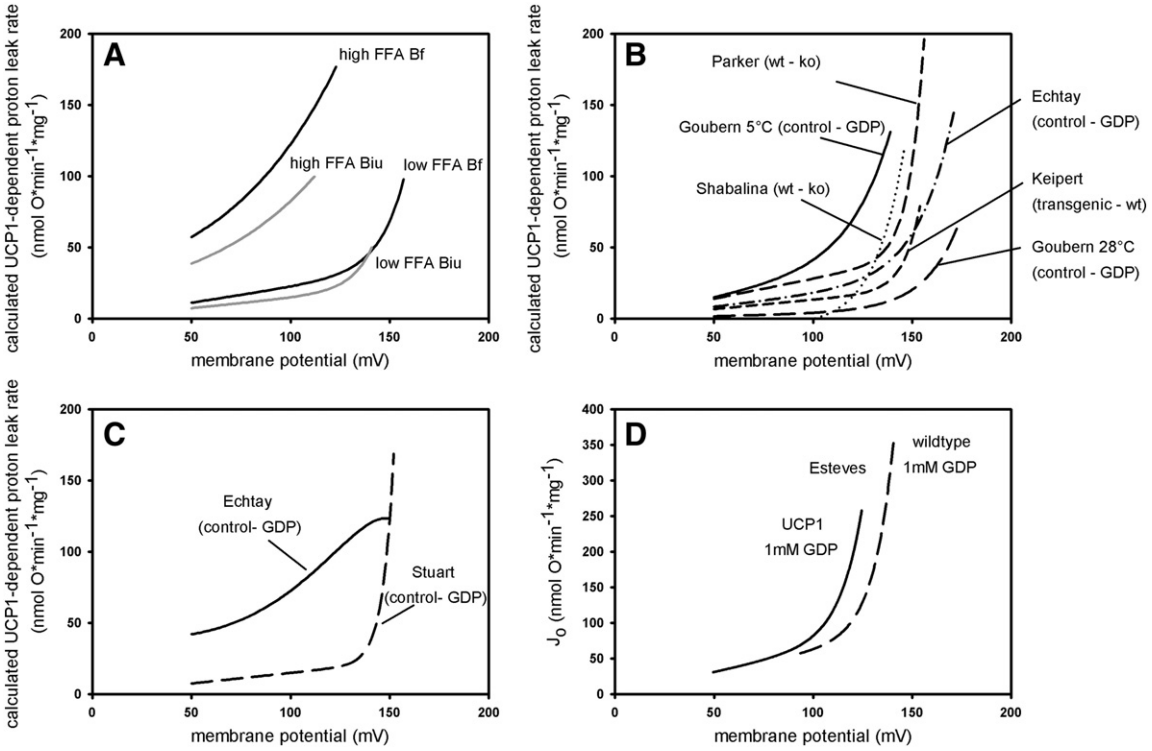

Fig. 8. UCP1-dependent proton leak rate of HEK293 UCP1 mitochondria and published data sets. Proton leak curves characterizing HEK293 cell mitochondria from this study (A), rat or mouse mitochondria (B) and yeast mitochondria (C, D) were subjected to regression analysis applying the term: $f(x) = a*x + b*\exp^{(c*x)}$. UCP1-dependent proton leak rate in the different models was calculated either by subtracting the regression equation of mitochondria without UCP1 from mitochondria containing UCP1 under the same experimental conditions or by subtracting the regression equation of mitochondria containing UCP1 in the presence of GDP from the curve in the absence of GDP. UCP1-dependent proton leak rate was plotted against membrane potential, illustrating that UCP1 activity increases almost linear at lower membrane potentials and exponentially when a critical membrane potential is reached. The value for this critical membrane potential is different depending on experimental conditions and the source of mitochondria. HEK293 cell mitochondria were quantified using the non-detergent Bradford method (Bf) which underestimates the protein content compared to most studies using detergents with the Biuret method (Biu). The illustration in (A) shows data quantified with Bf, and corrected for Biu. UCP1 activity displays study-to-study variation in animal mitochondria (B) and is highly variable in yeast data sets (C). Furthermore, basal proton leak of yeast mitochondria with inhibited UCP1 is higher than of wildtype mitochondria (D).

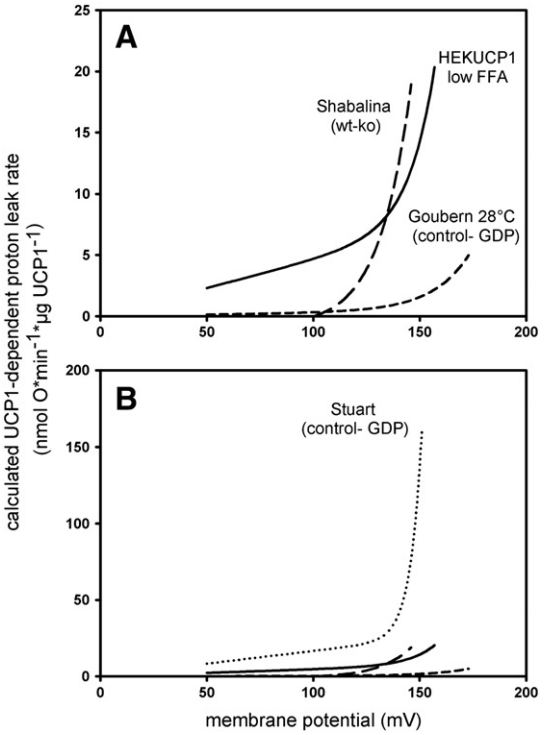

Fig. 9. Comparison of proton leak rates, normalised to UCP1 amount, of HEK293, brown adipose tissue and yeast mitochondria. (A) Normalised (nmol O min^{-1} mg^{-1} µg $UCP1^{-1}$) curves of the two extreme catalytic activities from brown adipose tissue mitochondria at low free fatty acid levels illustrate that the catalytic activity of HEK293 UCP1 is in this range at high membrane potentials. (B) The normalised activity of yeast UCP1 (here, the low activity study was chosen), is beyond the activities that are found for UCP1 in brown adipose tissue and HEK293 mitochondria.

lead to misfolded protein. Thus, expression of functional UCP1 in yeast appears not sufficiently robust for enzymologic studies. This can be also seen in a later study using the same UCP1-expressing vector in a different yeast strain: In the study by Esteves and colleagues [38], a high proportion of artificial uncoupling can be observed when comparing GDP-inhibited proton leak curves of UCP1-containing and wildtype yeast mitochondria (Fig. 8D). Furthermore, the activities of UCP1 in yeast appear to differ significantly between studies [19,29] (illustrated in Fig. 8C). A reason for differences in the upper limit of expression levels of functional UCP1 between yeast and HEK293 cells may originate from differences in mitochondrial inner membrane surface area. While this possibility should be further elaborated to identify reasons of differential handling of UCP1 overexpression, we here normalised our data conventionally to mitochondrial protein concentrations.

Whether UCP1 contributes to basal proton leak in its inhibited form is currently debated [11,12]. An unregulated leak by UCP1 could play a key role in obesity therapy considering the presence of functional brown adipose tissue in humans. Revisiting experiments conducted prior to the availability of the UCP1 knockout mouse model, BAT mitochondria of cold- and warm-acclimated guinea pigs expressing high and low levels of UCP1 showed no difference in proton conductance in the presence of GDP [3]. Comparing isolated mitochondria from UCP1-ablated and wildtype mice, no difference in basal proton conductance was observed measuring proton leak kinetics [39] or non-phosphorylating respiration in the presence of GDP [12,20]. In contrast to these studies, a higher proton conductance in wildtype vs. UCP1-ablated BAT mitochondria was found even when UCP1 was fully inhibited with GDP in the presence of 4% BSA [11]. Concerning previous studies, Parker et al. suggest that a different leakage by the ANT in the presence of different fatty acid concentrations, or a higher content of ANT2 in BAT [32] could account for a higher basal proton conductance in UCP1-ablated mice, hiding an increased UCP1-mediated basal proton leak. The experimental conditions in Parker et al. were criticised as BAT mitochondria from UCP1-ablated mice appear to be selectively damaged in low salt and 4% BSA medium [12]. Tissue mitochondria of mouse models that express UCP1 ectopically in skeletal muscle, heart and white adipose tissues did also not indicate contribution of UCP1 to basal proton leak. In this study, we refer to proton leak experiments of UCP1 in skeletal muscle mitochondria [30], which demonstrated no contribution of UCP1 to basal proton leak, similar to conclusions of an independently generated skeletal muscle/heart mouse line [40]. In a mouse line expressing UCP1 in white adipose tissue, mitochondrial membrane potential was estimated in digitonised adipocytes with TMRM and found to be lower as compared to wildtype adipocytes. Presence of BSA and GDP increased mitochondrial membrane potential to control levels [41].

In our HEK293 system, we found no evidence for UCP1 contributing to basal proton leak (Fig. 5). We used low BSA concentrations (0.3%) and excluded differences in ANT levels by CAT titration (Fig. 6). We considered that the UCP1 concentration in HEK293 mitochondria is about five times lower than in mice acclimated to room temperature. Therefore, UCP1 in HEK293 cells may not be directly comparable to mice due to lower UCP1 concentration. We would have expected, however, that UCP1-containing HEK293 mitochondria either doubled the basal proton leak rate or increased it by about 70 nmol H^+ (12 nmol O) mg^{-1} min^{-1} as compared to the wildtype controls. This calculation is based on 1) assuming linearity between UCP1 content and proton leak rate of the inhibited protein and 2) consulting the study by Parker et al., where the proton leak rate at about 153 mV was 6.5-fold higher in wildtype vs. UCP1-ablated mice, which translated into a proton leak rate of 365 nmol H^+ mg^{-1} min^{-1}. We conclude that the presence of properly folded and inserted UCP1 in HEK293 mitochondria does not contribute to basal proton leak and therefore agrees with studies stating no leakage of UCP1 in its inhibited form. In the UCP1-ablated mice, compensatory cellular mechanisms may influence the magnitude of basal proton leak. While this is less of a problem in HEK293 cells, we found that the ectopic expression of UCP1 significantly increased phosphorylating respiration but not maximum succinate oxidation (measured as FCCP-induced respiration). These findings hint towards an adjustment of the ATP synthase activity, possibly as a result of competition between proton motive force consuming processes of ATP synthesis and increased uncoupled respiration. The application of uncoupled respiration for the treatment of obesity, diabetes and age-related diseases has been suggested and negative side-effects extensively discussed in the past (reviewed in [10]). Beyond mechanistic studies on UCP1, the HEK293 cell system will also serve to study cellular adjustments upon treatment with mitochondrial uncoupling. We are pursuing to extend our studies on cellular adjustments in response to UCP1 expression.

In multiple studies, it can be observed that UCP1 activity is a function of mitochondrial membrane potential, but no mathematical relation has been addressed so far. We performed a regression analysis on the proton leak kinetics and UCP1 activity based on two hypotheses: a simple exponential relationship, as proposed by Garlid [34], as well as a function containing a second term that considers ohmic behaviour at low membrane potentials, as proposed by Nicholls [36] and other studies on current–voltage relationships of bilayer membranes. We found that $f(x) = ax + b * \exp^{(cx)}$ fitted our data points with a coefficient of determination of about 1, while data points at lower membrane potentials deviate stronger from a simple exponential equation. We therefore conclude that the kinetics of the proton leak follow overlaying ohmic and non-ohmic processes rather than solely non-ohmic behaviour. Based on various biophysical literature on current–voltage relationships of bilayer membranes, we are aware that 1) further correction parameters may be necessary to account for the complexity of processes at the mitochondrial inner membrane and 2) the ohmic behaviour of the lipid bilayer resistor at lower membrane potentials will transform into non-ohmic behaviour at higher potentials. However, a mathematical

confident description of the proton leak kinetics may have profound implications on future studies: We, and others, assumed linearity between two data points to calculate proton leak rate at fixed membrane potentials. While statistics consider variations in the proton leak rate, the deviation in the membrane potential has been broadly ignored. We emphasize that the use of mathematical proton leak functions may allow statistics for both dimensions, proton leak rate and mitochondrial membrane potential, in particular for very noisy data. To complete our regression analysis, we tested further functions of the proton leak. Three-factor exponentials ($f(x) = yo + a * \exp^{(bx)}$) fit well, but as yo deviates significantly from the origin, 3-factor exponential functions are not in accordance with the principles of the chemiosmotic theory [42]. Four-factor exponentials consider two overlaying non-ohmic processes, and are reasonable based on the Goldman-electrostatic barrier model. Although we found that the coefficient of determination was close to the ohmic/non-ohmic function for HEK293 mitochondria, our meta-analysis on data from selected publications revealed higher values of the coefficient of determination for $f(x) = ax + b * \exp^{(cx)}$ than for $f(x) = a * \exp^{(bx)} + c * \exp^{(dx)}$. Furthermore, there is no evidence assuming forward and backward reactions of proton leak justifying two exponential terms.

The ohmic/non-ohmic fit to our data may be false, as measurement of mitochondrial membrane potential with TPMP+ can be inaccurate at lower values. We verified our proton leak equation on data sets from different studies which used either TPMP+, rubidium+ or quenched safranine O. In all cases, we found the best fit for $f(x) = ax + b * \exp^{(cx)}$.

Applying $f(x) = ax + b * \exp^{(cx)}$ to all HEK293 cell proton leak curves facilitated the calculation of UCP1 activity as a function of membrane potential. We re-calculated the UCP1 catalytic centre activity based on the novel equation and found minor deviation from predicted values (shown in Table 1).

5. Conclusions

Analysis of the molecular mechanisms underlying UCP1 function is important for the understanding of protein activity, cellular and physiological integration, as well as for the identification of potential therapeutic targets. Caveats of conventional UCP test systems prompted us to characterize HEK293 cells as a novel mammalian system to study the function of UCP1. In this study, we show a) that UCP1 activity in HEK293 cells is similar to activities found in native mitochondria, and b) that UCP1 does not contribute to mitochondrial basal proton leak.

There is increasing evidence that active human brown adipose tissue benefits the treatment of diseases such as obesity and diabetes. Numerous approaches attempt to manipulate the mass of brown adipose tissue and UCP1 expression and protein levels while there is limited focus on activity. Activity of UCP1 in the physiological context is regulated by centrally controlled noradrenaline release and it appears that residual UCP1 activity is kept inhibited by purine nucleotides upon activation. Two issues arise when approaching UCP1 as a therapeutic target: first, when inducing UCP1 expression in tissues other than BAT — are these cells innervated for the activation of UCP1? Second, is there a possibility to circumvent central, peripheral and cellular control of UCP1 function by directly activating this mitochondrial protein to dissipate energy? In this study, we introduced a cellular system that is suitable to screen and characterize drugs that directly activate functional UCP1. Furthermore, we suggest that the HEK293 cell system is important for comparative studies on UCP paralogues (UCP2 and UCP3) and UCP1 orthologues.

Grants

This research was supported by the Deutsche Forschungsgemeinschaft (JA 1884/2-1; KL 973/7). VH was a member of the DFG graduate school 'Intra- and intercellular transport and communication' (GRK 1216).

Acknowledgements

Recombinant UCP1 standard was donated by B. Miroux.

Appendix A. Supplementary data

Supplementary data to this article can be found online at http://dx.doi.org/10.1016/j.bbabio.2012.05.014.

References

[1] D.G. Nicholls, R.M. Locke, Thermogenic mechanisms in brown fat, Physiol. Rev. 64 (1984) 1–64.
[2] J.M. Heaton, The distribution of brown adipose tissue in the human, J. Anat. 112 (1972) 35–39.
[3] R.M. Locke, E. Rial, D.G. Nicholls, The acute regulation of mitochondrial proton conductance in cells and mitochondria from the brown fat of cold-adapted and warm-adapted guinea pigs, Eur. J. Biochem. 129 (1982) 381–387.
[4] A. Bartelt, O.T. Bruns, R. Reimer, H. Hohenberg, H. Ittrich, K. Peldschus, M.G. Kaul, U.I. Tromsdorf, H. Weller, C. Waurisch, A. Eychmuller, P.L. Gordts, F. Rinninger, K. Bruegelmann, B. Freund, P. Nielsen, M. Merkel, J. Heeren, Brown adipose tissue activity controls triglyceride clearance, Nat. Med. 17 (2011) 200–205.
[5] A.M. Cypess, S. Lehman, G. Williams, I. Tal, D. Rodman, A.B. Goldfine, F.C. Kuo, E.L. Palmer, Y.H. Tseng, A. Doria, G.M. Kolodny, C.R. Kahn, Identification and importance of brown adipose tissue in adult humans, N. Engl. J. Med. 360 (2009) 1509–1517.
[6] W.D. van Marken Lichtenbelt, J.W. Vanhommerig, N.M. Smulders, J.M. Drossaerts, G.J. Kemerink, N.D. Bouvy, P. Schrauwen, G.J. Teule, Cold-activated brown adipose tissue in healthy men, N. Engl. J. Med. 360 (2009) 1500–1508.
[7] K.A. Virtanen, M.E. Lidell, J. Orava, M. Heglind, R. Westergren, T. Niemi, M. Taittonen, J. Laine, N.J. Savisto, S. Enerback, P. Nuutila, Functional brown adipose tissue in healthy adults, N. Engl. J. Med. 360 (2009) 1518–1525.
[8] P. Seale, B. Bjork, W. Yang, S. Kajimura, S. Chin, S. Kuang, A. Scime, S. Devarakonda, H.M. Conroe, H. Erdjument-Bromage, P. Tempst, M.A. Rudnicki, D.R. Beier, B.M. Spiegelman, PRDM16 controls a brown fat/skeletal muscle switch, Nature 454 (2008) 961–967.
[9] A. Vegiopoulos, K. Muller-Decker, D. Strzoda, I. Schmitt, E. Chichelnitskiy, A. Ostertag, D.M. Berriel, J. Rozman, A.M. Hrabe de, R.M. Nusing, C.W. Meyer, W. Wahli, M. Klingenspor, S. Herzig, Cyclooxygenase-2 controls energy homeostasis in mice by de novo recruitment of brown adipocytes, Science 328 (2010) 1158–1161.
[10] M. Jastroch, A.S. Divakaruni, S. Mookerjee, J.R. Treberg, M.D. Brand, Mitochondrial proton and electron leaks, Essays Biochem. 47 (2010) 53–67.
[11] N. Parker, P.G. Crichton, A.J. Vidal-Puig, M.D. Brand, Uncoupling protein-1 (UCP1) contributes to the basal proton conductance of brown adipose tissue mitochondria, J. Bioenerg. Biomembr. 41 (2009) 335–342.
[12] I.G. Shabalina, M. Ost, N. Petrovic, M. Vrbacky, J. Nedergaard, B. Cannon, Uncoupling protein-1 is not leaky, Biochim. Biophys. Acta 1797 (2010) 773–784.
[13] K.S. Echtay, E. Winkler, M. Bienengraeber, M. Klingenberg, Site-directed mutagenesis identifies residues in uncoupling protein (UCP1) involved in three different functions, Biochemistry 39 (2000) 3311–3317.
[14] T.C. Esteves, K.S. Echtay, T. Jonassen, C.F. Clarke, M.D. Brand, Ubiquinone is not required for proton conductance by uncoupling protein 1 in yeast mitochondria, Biochem. J. 379 (2004) 309–315.
[15] K.D. Garlid, D.E. Orosz, M. Modriansky, S. Vassanelli, P. Jezek, On the mechanism of fatty acid-induced proton transport by mitochondrial uncoupling protein, J. Biol. Chem. 271 (1996) 2615–2620.
[16] E. Winkler, M. Klingenberg, Effect of fatty acids on H^+ transport activity of the reconstituted uncoupling protein, J. Biol. Chem. 269 (1994) 2508–2515.
[17] P. Jezek, A.D. Costa, A.E. Vercesi, Reconstituted plant uncoupling mitochondrial protein allows for proton translocation via fatty acid cycling mechanism, J. Biol. Chem. 272 (1997) 24272–24278.
[18] M. Klingenberg, E. Winkler, The reconstituted isolated uncoupling protein is a membrane potential driven H^+ translocator, EMBO J. 4 (1985) 3087–3092.
[19] J.A. Stuart, J.A. Harper, K.M. Brindle, M.B. Jekabsons, M.D. Brand, A mitochondrial uncoupling artifact can be caused by expression of uncoupling protein 1 in yeast, Biochem. J. 356 (2001) 779–789.
[20] I.G. Shabalina, A. Jacobsson, B. Cannon, J. Nedergaard, Native UCP1 displays simple competitive kinetics between the regulators purine nucleotides and fatty acids, J. Biol. Chem. 279 (2004) 38236–38248.
[21] C.W. Meyer, M. Willershauser, M. Jastroch, B.C. Rourke, T. Fromme, R. Oelkrug, G. Heldmaier, M. Klingenspor, Adaptive thermogenesis and thermal conductance in wild-type and UCP1-KO mice, Am. J. Physiol. Regul. Integr. Comp. Physiol. 299 (2010) R1396–R1406.
[22] R. Oelkrug, M. Kutschke, C.W. Meyer, G. Heldmaier, M. Jastroch, Uncoupling protein 1 decreases superoxide production in brown adipose tissue mitochondria, J. Biol. Chem. 285 (2010) 21961–21968.
[23] P.G. Crichton, N. Parker, A.J. Vidal-Puig, M.D. Brand, Not all mitochondrial carrier proteins support permeability transition pore formation: no involvement of uncoupling protein 1, Biosci. Rep. 30 (2010) 187–192.
[24] P. Thomas, T.G. Smart, HEK293 cell line: a vehicle for the expression of recombinant proteins, J. Pharmacol. Toxicol. Methods 51 (2005) 187–200.
[25] L. Casteilla, O. Blondel, S. Klaus, S. Raimbault, P. Diolez, F. Moreau, F. Bouillaud, D. Ricquier, Stable expression of functional mitochondrial uncoupling protein in Chinese hamster ovary cells, Proc. Natl. Acad. Sci. U. S. A. 87 (1990) 5124–5128.

[26] J. Mozo, G. Ferry, A. Studeny, C. Pecqueur, M. Rodriguez, J.A. Boutin, F. Bouillaud, Expression of UCP3 in CHO cells does not cause uncoupling, but controls mitochondrial activity in the presence of glucose, Biochem. J. 393 (2006) 431–439.
[27] M. Klingenberg, K. Grebe, B. Scherer, The binding of atractylate and carboxyatractylate to mitochondria, Eur. J. Biochem. 52 (1975) 351–363.
[28] A.E. Adams, O.M. Kelly, R.K. Porter, Absence of mitochondrial uncoupling protein 1 affects apoptosis in thymocytes, thymocyte/T-cell profile and peripheral T-cell number, Biochim. Biophys. Acta 1797 (2010) 807–816.
[29] K.S. Echtay, D. Roussel, J. St-Pierre, M.B. Jekabsons, S. Cadenas, J.A. Stuart, J.A. Harper, S.J. Roebuck, A. Morrison, S. Pickering, J.C. Clapham, M.D. Brand, Superoxide activates mitochondrial uncoupling proteins, Nature 415 (2002) 96–99.
[30] S. Keipert, S. Klaus, G. Heldmaier, M. Jastroch, UCP1 ectopically expressed in murine muscle displays native function and mitigates mitochondrial superoxide production, Biochim. Biophys. Acta 1797 (2010) 324–330.
[31] S. Neschen, Y. Katterle, J. Richter, R. Augustin, S. Scherneck, F. Mirhashemi, A. Schurmann, H.G. Joost, S. Klaus, Uncoupling protein 1 expression in murine skeletal muscle increases AMPK activation, glucose turnover, and insulin sensitivity in vivo, Physiol. Genomics 33 (2008) 333–340.
[32] I.G. Shabalina, N. Petrovic, T.V. Kramarova, J. Hoeks, B. Cannon, J. Nedergaard, UCP1 and defense against oxidative stress. 4-Hydroxy-2-nonenal effects on brown fat mitochondria are uncoupling protein 1-independent, J. Biol. Chem. 281 (2006) 13882–13893.
[33] M.D. Brand, J.L. Pakay, A. Ocloo, J. Kokoszka, D.C. Wallace, P.S. Brookes, E.J. Cornwall, The basal proton conductance of mitochondria depends on adenine nucleotide translocase content, Biochem. J. 392 (2005) 353–362.
[34] K.D. Garlid, A.D. Beavis, S.K. Ratkje, On the nature of ion leaks in energy-transducing membranes, Biochim. Biophys. Acta 976 (1989) 109–120.
[35] H. Eyring, E.M. Eyring, Modern Chemical Kinetics, 1 ed. Van Nostrand Reinhold Inc., U.S., 1963
[36] D.G. Nicholls, The effective proton conductance of the inner membrane of mitochondria from brown adipose tissue. Dependency on proton electrochemical potential gradient, Eur. J. Biochem. 77 (1977) 349–356.
[37] J.W. Kauffman, C.A. Mead, Electrical characteristics of sphingomyelin bilayer membranes, Biophys. J. 10 (1970) 1084–1089.
[38] T.C. Esteves, N. Parker, M.D. Brand, Synergy of fatty acid and reactive alkenal activation of proton conductance through uncoupling protein 1 in mitochondria, Biochem. J. 395 (2006) 619–628.
[39] S. Monemdjou, L.P. Kozak, M.E. Harper, Mitochondrial proton leak in brown adipose tissue mitochondria of Ucp1-deficient mice is GDP insensitive, Am. J. Physiol. 276 (1999) E1073–E1082.
[40] E. Couplan, C. Gelly, M. Goubern, C. Fleury, B. Quesson, M. Silberberg, E. Thiaudiere, P. Mateo, M. Lonchampt, N. Levens, C. De Montrion, S. Ortmann, S. Klaus, M.D. Gonzalez-Barroso, A.M. Cassard-Doulcier, D. Ricquier, A.X. Bigard, P. Diolez, F. Bouillaud, High level of uncoupling protein 1 expression in muscle of transgenic mice selectively affects muscles at rest and decreases their IIb fiber content, J. Biol. Chem. 277 (2002) 43079–43088.
[41] F. Baumruk, P. Flachs, M. Horáková, D. Floryk, J. Kopecký, Transgenic UCP1 in white adipocytes modulates mitochondrial membrane potential, FEBS Lett. 444 (1999) 206–210.
[42] P. Mitchell, J. Moyle, Chemiosmotic hypothesis of oxidative phosphorylation, Nature 213 (1967) 137–139.